Finite amplitude thermal convection with variable gravity

D.N. Riahi

Department of Theoretical and Applied Mechanics

216 Talbot Laboratory, 104 S. Wright Street

University of Illinois at Urbana-Champaign, Urbana, Illinois 61801 U.S.A.

and

Albert T. Hsui

Department of Geology

245 Natural History Building, 1301 W. Green St.

University of Illinois at Urbana-Champaign, Urbana, Illinois 61801 U.S.A.

Abstract

Finite amplitude thermal convection is studied in a horizontal layer of infinite Prandtl number fluid with a variable gravity. For the present study, gravity is restricted to vary quadratically with respect to the vertical variable. A perturbation technique based on a small parameter, which is a measure of the ratio of the vertical to horizontal dimensions of the convective cells, is employed to determine the finite amplitude steady solutions. These solutions are represented in terms of convective modes whose amplitudes can be either small or of order unity. Stability of these solutions is investigated with respect to three dimensional disturbances. A variable gravity function introduces two non-dimensional parameters. For certain range of values of these two parameters, double or triple cellular structure in the vertical direction can be realized. Hexagonal patterns are preferred for sufficiently small amplitude of convection, while square patterns can become dominant for larger values of the convective amplitude. Variable gravity can also affect significantly the wavelength of the cellular pattern and the onset condition of the convective motion.

1 Introduction and Formulation

This paper studies the problem of finite amplitude convection in a horizontal layer of infinite Prandtl number fluid of depth d and bounded by two rigid plates subjected to a gravity function which varies quadratically with respect to the vertical variable z. Such a problem is of particular interest both in terms of fundamental knowledge and in terms of geological applications. Earth's mantle can be approximated as an infinite Prandtl number fluid because its viscosity is extremely large. In addition, the gravity field may vary as a function of radius only [1].

The present convection layer is assumed to be subjected to nearly insulating conditions at the top and bottom boundaries of the fluid layer. Such assumption is mainly for the mathematical convenience since, as was shown before [2], the governing system for such convection layer can be generalized and solved easily for cases where the coefficients of the terms in the governing equations vary with respect to the vertical variable z.

The present investigation is an extension of the small–amplitude theory to the finite–(but not necessarily small) amplitude regime, where the horizontal wave numbers $\alpha_n (n = 1, 2, \dots)$ that contribute to the horizontal planform functions satisfy the relationship

$$\alpha_n = \eta_n \gamma^{1/2}, \gamma \equiv (\beta/D)^{2/3} << 1, \tag{1}$$

where dD is the dimensional thickness of either horizontal rigid plate boundary, β is the ratio of thermal conductivity λ^e of the boundary to thermal conductivity λ of the fluid layer and the coefficients η_n are assumed to be of the order unity and independent of γ. This finite amplitude theory was developed by Riahi [3] in the context of a Marangoni convection problem and the reader is referred to this reference for details of the theory.

We consider an infinite horizontal layer of fluid of depth d bounded above and below by two infinite horizontal rigid plates of finite thickness dD and thermal conductivity λ^e. In the steady static state, a constant heat flux transverses the system such that the temperatures T_0 and $T_0 + \Delta T$ are attained at the upper and lower boundaries of the fluid. It is assumed that the gravity function $gG(z)$ varies quadratically with respect to the vertical variable z. Here the expression for $G(z)$ is normalized so that $\langle G(z) \rangle = 1$, where the angular bracket indicates an average over the fluid layer. We shall define the Rayleigh number R based on the constant g which is the average of the gravity function.

It is convenient to use non-dimensional variables in which length, velocity, time and temperature in the

fluid flow are scaled respectively by d, K/d, d^2/K and qd/R, where $q = \Delta T/[d(1 + 2D/\beta)]$ is the negative temperature gradient in the fluid (in the absence of fluid motion) and K is the thermal diffusivity of the fluid. Under the usual Boussinesq approximation, the non-dimensional forms of the equations for momentum, heat and conservation of mass can be simplified by using the representation

$$\boldsymbol{u} = \boldsymbol{\delta} v = \nabla \times \nabla \times \hat{\boldsymbol{z}} v, \tag{2}$$

for the divergence–free velocity vector $\boldsymbol{u}$. Here $\hat{\boldsymbol{z}}$ represents the unit vector in the vertical direction and v is the poloidal function for the velocity vector. The toroidal component $\nabla \times \hat{\boldsymbol{z}}\psi$ of $\boldsymbol{u}$ is not included in (2) since it can be shown that it is negligible in the limit of infinite Prandtl number P_r for the present analysis. Using (2), the vertical component of the double curl of the momentum equation in the limit of $P_r = \infty$ and the heat equation yield the following equations

$$\Delta_2 \left[\nabla^4 v - G(z)\theta\right] = 0, \tag{3a}$$

$$\nabla^2 \theta - R\Delta_2 v = \frac{\partial \theta}{\partial t} + \boldsymbol{\delta} v \cdot \nabla \theta, \tag{3b}$$

$$\frac{\partial \theta_e}{\partial t} = \mu \nabla^2 \theta_e, \tag{3c}$$

where θ and θ_e are the temperature fluctuations in the fluid layer and in the plates, $\mu = K_e/K$ is the ratio of the thermal diffusivity of the plates to that of the fluid, $R = agqd^4/(K\nu)$ is the Rayleigh number, a is the coefficient of thermal expansion, ν is the kinematic viscosity, t is the time variable, and Δ_2 is the horizontal Laplacian. The associated boundary conditions for (3) [2, 4] are

$$v = \frac{\partial v}{\partial z} = 0 \quad \text{at} \quad z = \pm\frac{1}{2}, \tag{4a}$$

$$\theta - \theta_e = \frac{\partial}{\partial z}(\theta - \beta\theta_e) = 0 \quad \text{at} \quad z = \pm\frac{1}{2}, \tag{4b}$$

$$\theta_e = 0 \quad \text{at} \quad z = \pm\left(\frac{1}{2} + D\right). \tag{4c}$$

Riahi [2] determined the boundary conditions for θ by solving (3c) and (4b)–(4c), subjected to the restriction that the thickness D of each plate is small in comparison to the horizontal dimension of the convection cells. Assuming the same restriction here, the boundary conditions for θ are [2]

$$\frac{\partial\theta}{\partial z} = \mp\gamma^2\theta \quad \text{at} \quad z = \pm\frac{1}{2}. \tag{5}$$

From previous studies [2, 4, 5] it is known that the predominant wave number in the horizontal direction vanishes when γ tends to zero. For the investigation of this limit we use γ as a perturbation parameter and anticipate that the relationship (1) holds in the limit of small γ.

In the next section we shall present the steady convection based on the system (3a)–(3b), (4a) and (5), where the gravity function is given by

$$G(z) = (1 - G_2/12) + G_1 z + G_2 z^2. \tag{6}$$

Here G_1 and G_2 are two constant parameters and $G(z)$ is normalized so that $\langle G(z)\rangle = 1$. Figure 1 presents some graphs of $G(z)$ versus z for cases where the extremum of $G(z)$ is a maximum, while Figure 2 presents some graphs of $G(z)$ versus z for cases where the extremum of $G(z)$ is a minimum.

2 Steady Convection

We start by introducing the horizontal planform function $w(x, y)$ that has the representation

$$w(x, y) = \sum_{m=1,n=-N_m}^{m=\infty,n=N_m} \varepsilon_m A_{nm} W_{nm}, \tag{7a}$$

$$W_{nm} = \exp(i\boldsymbol{k}_{nm} \cdot \boldsymbol{r}), \tag{7b}$$

and the function $w_m(x, y)$ defined by

$$w_m(x,y) = \sum_{n=-N_m}^{n=N_m} A_{nm} W_{nm} \tag{8a}$$

which satisfies the relation

$$\Delta_2 w_m + \alpha_m^2 w_m = 0, \quad \langle w_m^2 \rangle = 1. \tag{8b}$$

Here i is the imaginary number $\sqrt{-1}$, $\boldsymbol{r}$ is the position vector (x,y), ε_m is the amplitude of the mth mode and $\boldsymbol{k}_{nm}$ are the horizontal wave–number vectors for the mth mode that satisfy the properties

$$\boldsymbol{K}_{nm} \cdot \hat{\boldsymbol{z}} = 0, |\boldsymbol{K}_{nm}| = \alpha_m, \boldsymbol{K}_{nm} = -\boldsymbol{K}_{-nm}. \tag{9}$$

The coefficients A_{nm} satisfy the conditions

$$\sum_{n=-N_m}^{n=N_m} A_{nm} A_{nm}^* = 1, \quad A_{nm}^* = -A_{nm}, \tag{10}$$

where N_m denotes the number of horizontal wave–number vectors $\boldsymbol{K}_{nm}$ participating in the mth mode and the asterisk indicates the complex conjugate. The representation (7)–(10) given above are a generalization of representation in the small amplitude case [4] to those in the finite–(but not necessarily small) amplitude case.

The solutions of the steady state form of the governing system are obtained in terms of a series in powers of γ

$$(v, \theta, R) = \sum_{n=0} \gamma^n \left(v_n, \theta_n, R_n\right). \tag{11}$$

To $o(1)$, Eqs. (3a) and (3b) and the boundary conditions (4a) and (5) yield solutions of the form

$$(v_0, \theta_0) = [H_0(z), 1]\, w(x,y), \tag{12a}$$

where

$$H_0(z) = \left(z^2 - \frac{1}{4}\right)^2 \left[\frac{G_2}{3} z^2 + G_1 z + \left(5 - \frac{1}{4} G_2\right)\right] / 5!. \tag{12b}$$

In deriving the solutions a normalization condition of the form

$$\langle \theta_n \theta_0 \rangle = \delta_{no} \sum_m \varepsilon_m^2 \tag{13}$$

has been assumed. This condition has been used to determine the solution θ_n. Here $\delta_{n0} \equiv 1$ for $n = 0$ and zero otherwise.

The order γ system for Eqs. (3a)–(3b), (4a) and (5) yield solutions v_1 and θ_1. Averaging the equation for θ_1 over the fluid layer, we find

$$R_0 = 15120/(21 - G_2). \tag{14}$$

Here, R_0 has the value of 720 in the limit of $G_2 \to 0$ in agreement with the constant gravity result [4]. Multiplying the order γ^2 equation for θ_2 by W_{nl}, averaging over the fluid layer, and using order γ^2 boundary conditions, we find the following result:

$$-2\gamma\varepsilon_l A_{nl}^* + \langle W_{nl} \Delta_2 [\theta_1 - (R_1 v_0 + R_0 v_1)] \rangle = \langle W_{nl} (\delta v_0 \cdot \nabla \theta_1 + \delta v_1 \cdot \nabla \theta_0) \rangle. \tag{15}$$

Using (12) and solutions v_1 and θ_1 in (15), we find that (15) is a system of nonlinear algebraic equations for R_1 and the coefficients $A_{nl}(n = -N_n, \ldots, -1, 1, \ldots, N_n; l = 1, \ldots, \infty)$ as functions of N_l, η_l, flow pattern, and amplitudes ε_l. This system generally admits many different irregular and regular solutions [3]. As in the case of small amplitude theory [4], we restrict our analysis to the regular cases where the flow pattern is in the form of either rolls ($N_l = 1$), squares ($N_l = 2$), or hexagons ($N_l = 3$). Hence we apply the usual algebra and procedure [2] for simplifying the system (10) and (15). For dominant mode of convection with wave number α_l [3], it leads to the following results:

$$|A_{nl}|^2 = 1/(2N_l)(l = 1, \ldots, \infty), (n = 1, \ldots, N_l), \tag{16a}$$

$$R_1 = R_0(2\eta_l^{-2} + S_l \eta_l^2) \tag{16b}$$

where

$$S_l = B_0 + B_1 \varepsilon_l (\delta_{3N_l}) + B_2 \varepsilon_l^2, \tag{16c}$$

$$B_0 = (16.227 - 1.366G_2 - 0.184G_1^2 + 0.027G_2^2)/(21 - G_2)^2, \tag{16d}$$

$$B_1 = -\sqrt{6}G_1(0.173 + 0.016G_2)/(21 - G_2), \tag{16e}$$

$$\begin{aligned} B_2 = \{ \left(0.0334 + 0.0002G_1^2 + 0.0002G_2^2 - 0.0033G_2\right) + (1 - \delta_{1N_l}) \sum_{m=2}^{N_l} [\, (\, 0.0125 + 0.0001G_1^2 + \\ 0.0001G_2^2 - 0.0013G_2) + \left(0.0834 + 0.0002G_1^2 + 0.0002G_2^2 - 0.0080G_2\right) \phi_{m1}^2 \,] \, \} / (15120N_l), \end{aligned} \tag{16f}$$

$$\phi_{mn} = (\boldsymbol{K}_{ml} \cdot \boldsymbol{K}_{nl})/\alpha_l^2, \tag{16g}$$

and δ_{3N_l} is a Kronecker delta so that it equals one for $N_l = 3$ and zero otherwise. Minimizing the expression (16b) for R_1 with respect to η_l yields

$$R_{1p} = 2R_0(2S_l)^{1/2}, \eta_p = (2/S_l)^{1/4}, \tag{17}$$

where η_p designates the preferred η_l at which R_1 is minimized to R_{1p} with respect to the scaled wave number η_l. Using the approximate expression

$$R_1 = (R - R_0)/\gamma \tag{18}$$

for R_1 in (16b), we obtain the functional relationship between amplitude and wave number for the dominant mode and for given R, G_1 and G_2. Using (18) in the expression for R_{1p} given in (17), we obtain the expression for the preferred amplitude ε as a function of R, G_1, and G_2.

It should be noted from (16c) that depending on the sign of ε_l, the expression for S_l can either be given by the so-called subcritical form [3]

$$S_l^- = B_0 - |B_1||\varepsilon_l|\delta_{3N_l} + B_2\varepsilon_l^2. \tag{19a}$$

or by the so-called supercritical form [3]

$$S_l^+ = B_0 + |B_1||\varepsilon_l|\delta_{3N_l} + B_2\varepsilon_l^2. \tag{19b}$$

Here $S_l^- < S_l^+$ unless $N_l \neq 3$ or $|B_1| = 0$. Hence R_{1p} and η_p are given in terms of S_l^-. The expressions for S_l^- and S_l^+ are called subcritical and supercritical, respectively, with reference to the expression $B_0 + B_2\varepsilon_l^2$. Also, the flow due to the dominant mode is called subcritical flow if $S_l = S_l^-$ and supercritical flow if $S_l = S_l^+$ [3].

For either subcritical or supercritical flow case, the corresponding flow pattern is that due to hexagonal cells, and we can find the sign of the vertical motion, at any plane $z = z_0$, $|z_0| < \frac{1}{2}$, at the cells' center $r = 0$ by the following procedure. We have

$$u_3 = \boldsymbol{u} \cdot \hat{z} \backsimeq \frac{\gamma}{\sqrt{6}} H_0(z_0)\varepsilon_l\eta_l^2 \quad \text{at} \quad r = 0, z = z_0. \tag{20}$$

Hence, u_3 at $z = z_0$ and $r = 0$ has the same sign as $H_0\varepsilon_l$. Since the minimum state (17) is due to the subcritical flow for $N_l = 3$, the subcritical hexagons are preferred over the supercritical hexagons. If u_3 given by (20) is negative, then the subcritical hexagons are called down-hexagons, while for $u_3 > 0$ such hexagons are called up-hexagons.

Using the approximate expression

$$H_c = \langle \theta u_3 \rangle \backsimeq -\langle \theta_0 \Delta_2 v_0 \rangle = \gamma\varepsilon_l^2\eta_l^2 \tag{21}$$

for the heat transported by convection, the results (17) and (18) can be used to determine the expression for H_c as function of R, γ, G_1 and G_2. For the case of convection in the form of two-dimensional rolls, $N_l = 1$, we find

$$H_c = \frac{4|R_0|\gamma^2}{|(R - R_0)|}\left[\frac{(R - R_0)^2}{8R_0^2\gamma^2} - B_0\right]\left(\frac{1}{\frac{B_3}{2} + B_4}\right), \tag{22a}$$

where

$$B_3 = (0.0417 + 0.0001G_1^2 + 0.0001G_2^2 - 0.0040G_2)/15120, \tag{22b}$$

$$B_4 = (0.0125 + 0.0001G_1^2 + 0.0001G_2^2 - 0.0013G_2)/15120. \tag{22c}$$

For the case of square pattern convection, $N_l = 2$, we find

$$H_c = \frac{4|R_0|\gamma^2}{|(R-R_0)|}\left[\frac{(R-R_0)^2}{8R_0^2\gamma^2} - B_0\right]\left(\frac{1}{\frac{B_3}{4}+B_4}\right). \tag{23}$$

Detailed computations indicate that $B_3 = \langle H_0^2 \rangle$, so that $B_3 > 0$ as (22b) also indicates. Hence, comparing (22a) and (23), we find that square cells transport more heat than rolls for all possible values of G_1 and G_2. For the case of hexagon pattern convection, $N_l = 3$, we find the following result for the preferred subcritical hexagons:

$$H_c = \frac{|R_0|\gamma^2}{B_5^2|(R-R_0)|}\left\{|B_1| + \frac{B_5}{|B_5|}\sqrt{B_1^2 + 4B_5\left[\frac{(R-R_0)^2}{8R_0^2\gamma^2} - B_0\right]}\right\}^2, B_5 \equiv \frac{B_3}{2} + B_4. \tag{24}$$

Using (17) and (18), we obtain the following expression for the preferred wavelength $L_p = 2\pi/(\eta_p\sqrt{\gamma})$:

$$L_p = \pi\sqrt{|R-R_0|}/(\gamma\sqrt{|R_0|}). \tag{25}$$

3 Stability Analysis

We now investigate the stability of the steady solutions that were determined in the previous section. The equations for the time dependent disturbances $\tilde{v}$ and $\tilde{\theta}$ are given by

$$\Delta_2(\nabla^4\tilde{v} - G\tilde{\theta}) = 0, \tag{26a}$$

$$(\nabla^2 - \sigma)\tilde{\theta} - R\Delta_2\tilde{\theta} = \delta\tilde{v}\cdot\nabla\theta + \delta v\cdot\nabla\tilde{\theta}, \tag{26b}$$

where the growth rate σ is defined by $\frac{\partial}{\partial t} = \sigma$. The boundary conditions for $\tilde{v}$ and $\tilde{\theta}$ are the same as those for v and θ, respectively, so that

$$v = \frac{\partial v}{\partial z} = \left(\frac{\partial}{\partial z} \pm \gamma^2\right)\tilde{\theta} = 0 \quad \text{at} \quad z = \pm\frac{1}{2}. \tag{26c}$$

The system (26) is solved by using the following perturbation expansion:

$$\left(\tilde{v},\tilde{\theta},\sigma\right)=\sum_{n=0}\gamma^{n}\left(\tilde{v}_{n},\tilde{\theta}_{n},\sigma_{n}\right). \tag{27}$$

To $o(1)$ equations (26a)-(26b) and the boundary conditions (26c) are of the same form as the corresponding ones for the steady finite amplitude case. The solutions are

$$\tilde{v}_0 = H_0(z)\tilde{w}(x,y), \tilde{\theta}_0 = \tilde{w}(x,y), \sigma_0 = 0, \tag{28a}$$

where

$$\tilde{w}(x,y)=\sum_{n=-\infty}^{n=\infty}\tilde{A}_n\tilde{w}_n, \tilde{w}_n=\exp(i\tilde{\boldsymbol{k}}_n\cdot\boldsymbol{r}). \tag{28b}$$

Here, $\tilde{w}(x,y)$ is the horizontal planform function of the general three-dimensional disturbances, $\tilde{A}_n$ are constant coefficients, $\tilde{\boldsymbol{k}}_n$ are the horizontal wave number vectors of disturbances which satisfy the properties

$$\tilde{\boldsymbol{k}}_n\cdot\hat{z}=0, \quad |\tilde{\boldsymbol{k}}_m|=\tilde{\alpha}_n-\tilde{\eta}_n\gamma^{\frac{1}{2}}, \quad \tilde{\boldsymbol{k}}_n=-\tilde{\boldsymbol{k}}_{-n}, \tag{28c}$$

and the parameters $\tilde{\eta}_n$ are assumed to be at most of the order unity and independent of γ.

The order γ system for the governing equations (26a)-(26b) and boundary conditions (26c) yields solutions $\tilde{v}_1$ and $\tilde{\theta}_1$. The solvability condition for the order γ system then yields

$$\sigma_1 = 0. \tag{29}$$

Multiplying the order γ^2 equation for $\tilde{\theta}_2$ by $\tilde{w}_n$, averaging over the fluid layer, and using order γ^2 boundary conditions, we find the following result:

$$\begin{aligned}-\gamma A_n^*(2+\sigma_2)+\langle\tilde{w}_n\Delta_2\left[\tilde{\theta}_1-(R_1\tilde{v}_0+R_0\tilde{v}_1)\right]\rangle=\\ \langle\tilde{w}_n\left[\boldsymbol{\delta}\tilde{v}_0\cdot\nabla\theta_1+\boldsymbol{\delta}v_0\cdot\nabla\tilde{\theta}_1+\boldsymbol{\delta}\tilde{v}_1\cdot\nabla\theta_0+\boldsymbol{\delta}v_1\cdot\nabla\tilde{\theta}_0\right]\rangle.\end{aligned} \tag{30}$$

Using (12), (28), and the solution $v_1, \theta_1, \tilde{v}_1$, and $\tilde{\theta}_1$ in (30), we find that (30) is a system of algebraic equations for σ_2 and the coefficients $\tilde{A}_n$. Here, the procedure to determine the growth rates σ_2 is similar to those used in [6] and [2]. Rather than repeating that procedure for deriving the eigenvalues σ_2 of (30), we refer the

reader to these references for further details. Following Riahi [2], we find that the only possible stable solutions are those of subcritical hexagons and squares. Square pattern convection is found to be stable for

$$|\varepsilon_l| \geq 12|B_1|/(\sqrt{6}B_3), \tag{31a}$$

while subcritical hexagon pattern convection is found to be stable for

$$|\varepsilon_l| \geq 2|B_1|/|(B_3 + 2B_4)|. \tag{31b}$$

In addition, present analysis is valid, provided

$$|\varepsilon_l| << \gamma^{-1} \tag{32}$$

[4].

4 Discussion of the results

Before discussing the results obtained in the last two sections, it is of interest to discuss the structure of the quadratic form of the gravity function $G(z)$ given by (6). Due to such quadratic form of $G(z)$, we assume that

$$G_2 \neq 0. \tag{33a}$$

The function $G(z)$ has an extremum at

$$z = -G_1/(2G_2). \tag{33b}$$

This extremum is a minimum for

$$G_2 > 0 \tag{33c}$$

and is a maximum for

$$G_2 < 0. \tag{33d}$$

The extremum of $G(z)$ lies in the layer interval $|z| < 1/2$ for

$$-1 < -G_1/G_2 < 1. \tag{33e}$$

The function $G(z)$ is symmetric with respect to its extremum value if

$$G_1 = 0 \tag{33f}$$

and asymmetric otherwise. See figures 1 and 2 which agree with the above analytical features.

The z-dependence $H_0(z)$ of the leading order term for the vertical component $u_3 = -\Delta_2 v_0$ of the velocity vector, given by (12b) indicate that it can vanish once or twice within the layer interval $|z| < 1/2$, provided

$$|-(3G_1/G_2) + \left[9(G_1/G_2)^2 + (3 - 60/G_2)\right]^{1/2}| < 1 \tag{34a}$$

and/or

$$|-(3G_1/G_2) - \left[9(G_1/G_2)^2 + (3 - 60/G_2)\right]^{1/2}| < 1. \tag{34b}$$

The fluid layer can then be composed of double or triple cell structures in the vertical direction with different flow direction in each set of cells at given r values. For example, double-layer structure can exist for $G_1 = 12.$ and $G_2 = -3.$ (figure 1), while triple-layer structure can exist for $G_1 = -5/3$ and $G_2 = 20$ (figure 2).

The expression (14) for R_0 indicates that the effect of G_2 is destabilizing for $G_2 < 0$ and stabilizing for $G_2 > 0$, and R_0 is independent of G_1. The expressions (16b),(16c) and (18) indicate the functional relationship between ε_l and η_l for given R, γ, G_1 and G_2. Thus the dominant mode with certain amplitude allows particular wavelength. Of particular interest is the preferred mode represented by (17) where the expression for R_1 is minimized with respect to the wavelength. Using (16c), (17) and (18), we find that the amplitude $|\varepsilon_p|$ for the preferred mode can increase with R, for given γ, G_1 and G_2, provided

$$\left[|B_1|\delta_{3N_l} + (R - R_0)/(2\gamma R_0)^2\right]/B_2 > 0. \tag{35}$$

Furthermore, (16c) and (17) indicate that the preferred wavelength of the convection cells depend strongly on the gravity parameters G_1 and G_2. For example, for small $|\varepsilon_l|$ case, η_p is smaller than the corresponding value 3.006, which is realized in the absence of variable $G(G_1 = G_2 = 0)$, provided $|G_1|$ is sufficiently small and G_2 lies in the range

$$0 < G_2 < 18.312. \tag{36}$$

However, if $|G_2|$ is sufficiently small and $|G_1|$ is sufficiently large, then $\eta_p > 3.006$. It should be noted from (16c) and (17) that the present theory breaks down if S_l becomes negative. Hence, the condition for the validity of the present results is that

$$B_2|\varepsilon_l|^2 - |B_1||\varepsilon_l|\delta_{3N_l} + B_0 > 0. \tag{37}$$

The expression for R_{1p} in (17) indicates that there is no finite amplitude instability for $R_0 > 0$, but there is such instability for $R_0 < 0$. However, for the small amplitude case, stable flow can be shown to be subcritically operative. Such subcritical behavior is found to exist for hexagons if either

$$G_1(2.076 + 0.192G_2) < 0 \quad \text{for} \quad \varepsilon_l < 0 \tag{38a}$$

or

$$G_1(2.076 + 0.192G_2) > 0 \quad \text{for} \quad \varepsilon_l > 0 \tag{38b}$$

Similar subcritical behavior is exhibited by squares if

$$G_2 > 25.3 + 6.24(1 + 0.18G_1^2)^{1/2}. \tag{38c}$$

Hence subcritical instability can exist only in a small range of R where amplitude of motion is sufficiently small. For large amplitudes second order terms in ε_l in (16c) dominates over lower order terms in ε_l resulting in a positive R_1 given by (16b).

To discuss the direction of motion at the cells' center in a sub-layer where $H_0(z)$ has only one sign, we restrict the discussion for the hexagonal cells only since it is known [7] that a change of sign of motion at the cells' center can lead to qualitatively different cellular structures only in the case of hexagons. Thus we consider the expression (20) for u_3 at $z = z_0(|z_0| < \frac{1}{2})$ and note that it satisfies the condition

$$u_3 H_0(z)\varepsilon_l > 0. \tag{39a}$$

We already found that stable subcritical hexagons are those for which the condition

$$B_1\varepsilon_l < 0. \tag{39b}$$

Given G_1 and G_2, B_1 has a definite sign implying that ε_l has one sign opposite to that of B_1. Thus, it follows that $H_0(z)$ has a definite sign. Consequently, the sign of u_3 can be found easily. For example, if $z_0 = 0$, $0 < G_2 < 20$ and $G_1 > 0$, then $H_0(z_0) > 0$, $B_1 < 0$ and $\varepsilon_l > 0$. Hence $u_3 > 0$ and motion is upward at the hexagons' center and at the mid-plane $z = 0$. For $z_0 = 0$ and $0 < G_2 < 20$ and $G_1 < 0$, then $H_0(z_0) > 0$, $B_1 > 0$ and $\varepsilon_l < 0$. Hence $u_3 < 0$ and motion is downward at the hexagons' center and at the mid-plane $z = 0$. The results for the sign of motion appears to be independent of the magnitudes of the amplitudes. For the case $B_1 = 0$, the flow direction can be discussed if S_l is modified by inclusion of the results to the order γ^3 in the governing equations.

The expressions (22)-(24) for heat transported by convection, due to rolls, squares and hexagons, provide dependence of the heat flux on R, γ, G_1 and G_2. Since η_l and R_1 change abruptly if the flow pattern changes, we expect that the heat flux changes abruptly if the convection pattern changes due to a bifurcation. Also a non-monotonicity of the heat flux with respect to G_1 and G_2 for a given R cannot be ruled out.

The preferred wavelength L_p of the stable convection cells given by (25) indicate that L_p increases with R for given G_2. It is independent of G_1 since R_0 does not depend on G_1.

The stability conditions (31a)-(31b) indicate that although small amplitude theory may be adequate for small $|G_1|$ where the right hand sides of (31a) and (31b) can become small compared to unity, it certainly is not adequate for large $|G_1|$ which require at least order one values for $|\varepsilon_l|$.

It can be deduced from the expression (16f) for B_2 that $B_2 > 0$ for both stable squares and subcritical hexagons. Using this result and the stability conditions (31a,b) in the expression (16c) for S_l, we can compare η_p, given in (17), to the corresponding η_c, defined by

$$\eta_c = (2/B_0)^{1/4}, \tag{40}$$

which is the critical η at which convection first occurs as R is increased. We find

$$\eta_p < \eta_c, \tag{41}$$

and note that $|\eta_p - \eta_c|$ increases with ε_l, and η_p is very close to η_c for small amplitude case. These results are in agreement with the corresponding ones obtained by Proctor [8] and Riahi [3] in the case of uniform gravity ($G \equiv 1$).

Small amplitude convection with variable properties and internal heating was investigated by Riahi [9] using small amplitude theory of Busse and Riahi [4]. Riahi finds, in particular, that his general qualitative results depend on the symmetries and anti-symmetries of the variable properties and internal heating functions with respect to the mid-plane of the fluid layer. Results of the present investigation are in general agreement with his results regarding unstable rolls and possible stable squares or hexagons.

References

[1] S. Chandrasekhar, Hydrodynamic and Hydromagnetic Stability, Oxford University Press, (1961).

[2] N. Riahi, Nonlinear convection in a horizontal layer with an internal heat source, *J. Phys. Soc. Japan* **53**, 4169-4178 (1984).

[3] D.N. Riahi, Hexagon pattern convection for Bénard-Marangoni problem, *Int. J. Engrg. Sci.* **27**, 689-700 (1989).

[4] F.H. Busse and N. Riahi, Nonlinear convection in a layer with nearly insulating boundaries, *J. Fluid Mech.* **96**, 243-256 (1980).

[5] N. Riahi, Nonlinear convection in a porous layer with finite conducting boundaries, *J. Fluid Mech.* **129**, 153-171 (1983).

[6] F.H. Busse, The stability of finite amplitude cellular convection and its relation to an extremum principle, *J. Fluid Mech.* **30**, 625-649 (1967)

[7] F.H. Busse, Nonlinear properties of thermal convection, *Rep. Prog. Phys.*, **41**, 1929-1967 (1978).

[8] M.R.E. Proctor, Planform selection by finite–amplitude thermal convection between poorly conducting slabs, *J. Fluid Mech.* **113**, 469-485 (1981).

[9] D.N. Riahi, Nonlinear convection with variable properties and internal heating, *J. Math. Phys. Sci.* **22**, 161-180 (1988).

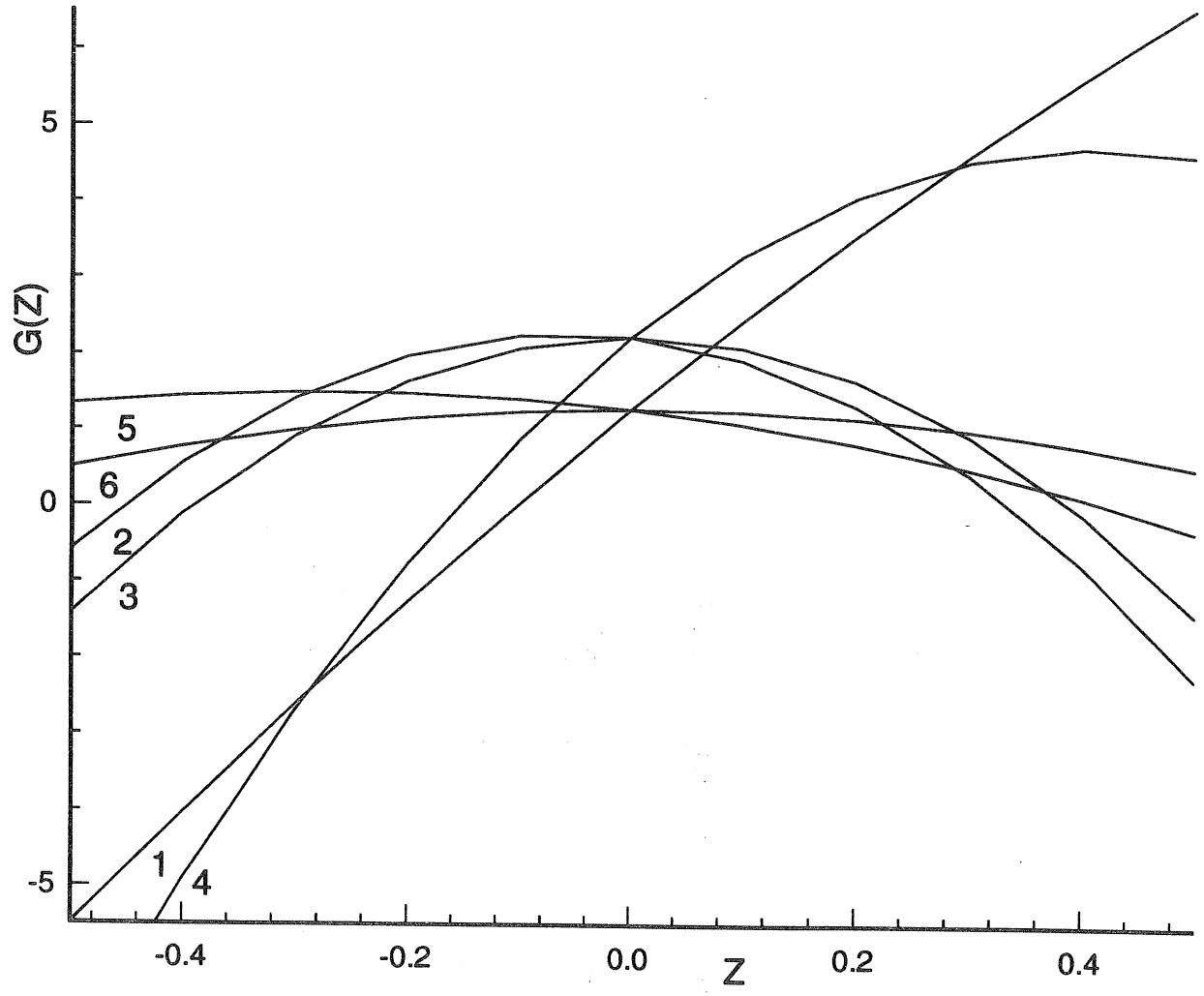

Figure 1: The gravity function $G(z)$ versus z for $G_2 < 0$. Each curve is labeled by a number given just below the curve. The curves 1, 2 and 3 are for G_2=-14.5 and correspond, respectively, to $G_1 = -5/3$, 0.0 and 12.0. The curves 4, 5 and 6 are for G_2=-3.0 and correspond, respectively, to G_1=-5/3, 0.0 and 12.0.

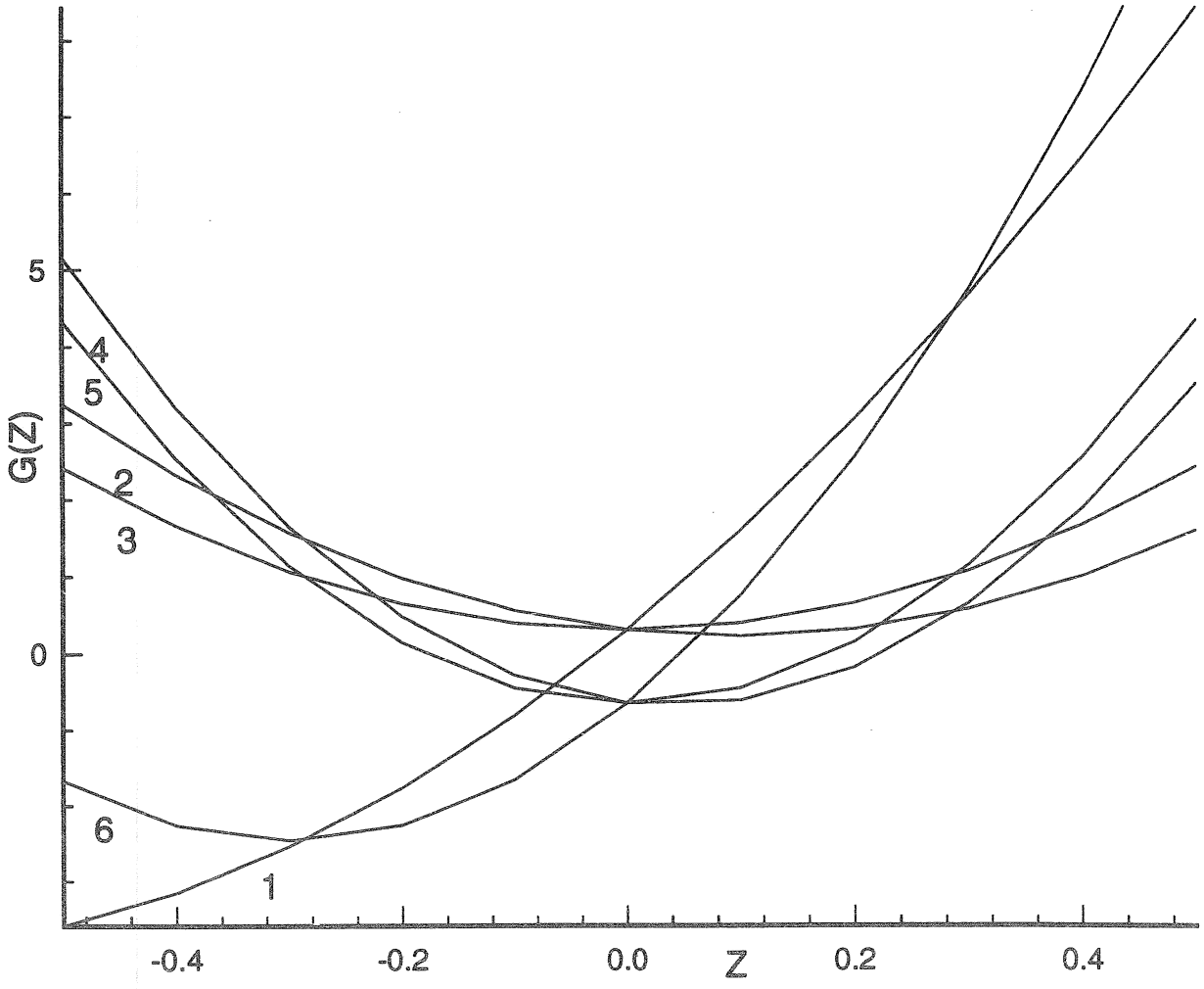

Figure 2: The gravity function $G(z)$ versus z for $G_0 > 0$. Each curve is labeled by a number given just below the curve. The curves 1,2 and 3 are for G_2=8.5 and correspond, respectively to G_1=-5/3, 0. and 12.0. The curves 4, 5 and 6 are for G_2 =20.0 and correspond, respectively, to G_1=-5/3, 0.0 and 12.0.

List of Recent TAM Reports

No.	Authors	Title	Date
833	Riahi, D. N.	Effect of centrifugal and Coriolis forces on chimney convection during alloy solidification—*Journal of Crystal Growth* **179** , 287–296 (1997)	Sept. 1996
834	Cermelli, P., and E. Fried	The influence of inertia on configurational forces in a deformable solid—*Proceedings of the Royal Society of London A* **453**, 1915–1927 (1997)	Oct. 1996
835	Riahi, D. N.	On the stability of shear flows with combined temporal and spatial imperfections	Oct. 1996
836	Carranza, F. L., B. Fang, and R. B. Haber	An adaptive space–time finite element model for oxidation-driven fracture, *Computer Methods in Applied Mechanics and Engineering*, in press (1997)	Nov. 1996
837	Carranza, F. L., B. Fang, and R. B. Haber	A moving cohesive interface model for fracture in creeping materials, *Computational Mechanics* **19**, 517–521 (1997)	Nov. 1996
838	Balachandar, S., R. Mittal, and F. M. Najjar	Properties of the mean wake recirculation region in two-dimensional bluff body wakes—*Journal of Fluid Mechanics*, in press (1997)	Dec. 1996
839	Ti, B. W., W. D. O'Brien, Jr., and J. G. Harris	Measurements of coupled Rayleigh wave propagation in an elastic plate—*Journal of the Acoustical Society of America* **102**, 1528–1531	Dec. 1996
840	Phillips, W. R. C.	On finite-amplitude rotational waves in viscous shear flows—*Studies in Applied Mathematics* **100**, in press (1998)	Jan. 1997
841	Riahi, D. N.	Direct resonance analysis and modeling for a turbulent boundary layer over a corrugated surface—*Acta Mechanica* **131**, 225–233 (1998)	Jan. 1997
842	Liu, Z.-C., R. J. Adrian, C. D. Meinhart, and W. Lai	Structure of a turbulent boundary layer using a stereoscopic, large format video-PIV—*Developments in Laser Techniques and Fluid Mechanics*, 259–273 (1997)	Jan. 1997
843	Fang, B., F. L. Carranza, and R. B. Haber	An adaptive discontinuous Galerkin method for viscoplastic analysis—*Computer Methods in Applied Mechanics and Engineering* **150**, 191–198 (1997)	Jan. 1997
844	Xu, S., T. D. Aslam, and D. S. Stewart	High-resolution numerical simulation of ideal and non-ideal compressible reacting flows with embedded internal boundaries—*Combustion Theory and Modeling* **1**, 113–142 (1997)	Jan. 1997
845	Zhou, J., C. D. Meinhart, S. Balachandar, and R. J. Adrian	Formation of coherent hairpin packets in wall turbulence—In *Self-Sustaining Mechanisms in Wall Turbulence*, R. L. Panton, ed. Southampton, UK: Computational Mechanics Publications, 109–134 (1997)	Feb. 1997
846	Lufrano, J. M., P. Sofronis, and H. K. Birnbaum	Elastoplastically accommodated hydride formation and embrittlement—*Journal of Mechanics and Physics of Solids*, in press (1998)	Feb. 1997
847	Keane, R. D., N. Fujisawa, and R. J. Adrian	Unsteady non-penetrative thermal convection from non-uniform surfaces—In *Geophysical and Astrophysical Convection*, R. Kerr, ed. (1997)	Feb. 1997
848	Aref, H., and M. Brøns	On stagnation points and streamline topology in vortex flows—*Journal of Fluid Mechanics* **370**, 1–27 (1998)	Mar. 1997
849	Asghar, S., T. Hayat, and J. G. Harris	Diffraction by a slit in an infinite porous barrier—*Wave Motion*, in press (1998)	Mar. 1997
850	Shawki, T. G., H. Aref, and J. W. Phillips	Mechanics on the Web—Proceedings of the International Conference on Engineering Education (Aug. 1997, Chicago)	Apr. 1997
851	Stewart, D. S., and J. Yao	The normal detonation shock velocity–curvature relationship for materials with non-ideal equation of state and multiple turning points—*Combustion* **113**, 224–235 (1998)	Apr. 1997
852	Fried, E., A. Q. Shen, and S. T. Thoroddsen	Wave patterns in a thin layer of sand within a rotating horizontal cylinder—*Physics of Fluids* **10**, 10–12 (1998)	Apr. 1997
853	Boyland, P. L., H. Aref, and M. A. Stremler	Topological fluid mechanics of stirring—*Bulletin of the American Physical Society* **41**, 1683 (1996)	Apr. 1997

List of Recent TAM Reports (cont'd)

No.	Authors	Title	Date
854	Parker, S. J., and S. Balachandar	Viscous and inviscid instabilities of flow along a streamwise corner—*Bulletin of the American Physical Society* **42**, 2155 (1997)	May 1997
855	Soloff, S. M., R. J. Adrian, and Z.-C. Liu	Distortion compensation for generalized stereoscopic particle image velocimetry—*Measurement Science and Technology* **8**, 1–14 (1997)	May 1997
856	Zhou, Z., R. J. Adrian, S. Balachandar, and T. M. Kendall	Mechanisms for generating coherent packets of hairpin vortices in near-wall turbulence—*Bulletin of the American Physical Society* **42**, 2243 (1997)	June 1997
857	Neishtadt, A. I., D. L. Vainshtein, and A. A. Vasiliev	Chaotic advection in a cubic stokes flow—*Physica D* **111**, 227 (1997).	June 1997
858	Weaver, R. L.	Ultrasonics in an aluminum foam—*Ultrasonics* **36**, 435–442 (1998)	July 1997
859	Riahi, D. N.	High gravity convection in a mushy layer during alloy solidification—In *Nonlinear Instability, Chaos and Turbulence*, D. N. Riahi and L. Debnath, eds., **1**, 301–336 (1998)	July 1997
860	Najjar, F. M., and S. Balachandar	Low-frequency unsteadiness in the wake of a normal plate, *Bulletin of the American Physical Society* **42**, 2212 (1997)	Aug. 1997
861	Short, M.	A parabolic linear evolution equation for cellular detonation instability—*Combustion Theory and Modeling* **1**, 313–346 (1997)	Aug. 1997
862	Short, M., and D. S. Stewart	Cellular detonation stability, I: A normal-mode linear analysis—*Journal of Fluid Mechanics* **368**, 229–262 (1998)	Sept. 1997
863	Carranza, F. L., and R. B. Haber	A numerical study of intergranular fracture and oxygen embrittlement in an elastic–viscoplastic solid—*Journal of the Mechanics and Physics of Solids*, in press (1997)	Oct. 1997
864	Sakakibara, J., and R. J. Adrian	Whole-field measurement of temperature in water using two-color laser-induced fluorescence—*Experiments in Fluids* **26**, 7–15 (1999)	Oct. 1997
865	Riahi, D. N.	Effect of surface corrugation on convection in a three-dimensional finite box of fluid-saturated porous material—*Theoretical and Computational Fluid Dynamics*, in press (1999)	Oct. 1997
866	Baker, C. F., and D. N. Riahi	Three-dimensional flow instabilities during alloy solidification	Oct. 1997
867	Fried, E.	Introduction (only) to *The Physical and Mathematical Foundations of the Continuum Theory of Evolving Phase Interfaces* (book containing 14 seminal papers dedicated to Morton E. Gurtin), Berlin: Springer-Verlag, in press (1998)	Oct. 1997
868	Folguera, A., and J. G. Harris	Coupled Rayleigh surface waves in a slowly varying elastic waveguide—*Proceedings of the Royal Society of London*, in press (1998)	Oct. 1997
869	Stewart, D. S.	Detonation shock dynamics: Application for precision cutting of metal with detonation waves	Oct. 1997
870	Shrotriya, P., and N. R. Sottos	Creep and relaxation behavior of woven glass/epoxy substrates for multilayer circuit board applications—*Polymer Composites* **19**, 567–578 (1998)	Nov. 1997
871	Riahi, D. N.	Boundary wave–vortex interaction in channel flow at high Reynolds numbers, *Fluid Dynamics Research* **25**, 129–145 (1999)	Nov. 1997
872	George, W. K., L. Castillo, and M. Wosnik	A theory for turbulent pipe and channel flows—paper presented at *Disquisitiones Mechanicae* (Urbana, Ill., October 1996)	Nov. 1997
873	Aslam, T. D., and D. S. Stewart	Detonation shock dynamics and comparisons with direct numerical simulation—*Combustion Theory and Modeling*, in press (1999)	Dec. 1997
874	Short, M., and A. K. Kapila	Blow-up in semilinear parabolic equations with weak diffusion	Dec. 1997
875	Riahi, D. N.	Analysis and modeling for a turbulent convective plume—*Mathematical and Computer Modeling* **28**, 57–63 (1998)	Jan. 1998
876	Stremler, M. A., and H. Aref	Motion of three point vortices in a periodic parallelogram—*Journal of Fluid Mechanics* **392**, 101-128 (1999)	Feb. 1998

List of Recent TAM Reports (cont'd)

No.	*Authors*	*Title*	*Date*
877	Dey, N., K. J. Hsia, and D. F. Socie	On the stress dependence of high-temperature static fatigue life of ceramics	Feb. 1998
878	Brown, E. N., and N. R. Sottos	Thermoelastic properties of plain weave composites for multilayer circuit board applications	Feb. 1998
879	Riahi, D. N.	On the effect of a corrugated boundary on convective motion—*Journal of Theoretical and Applied Mechanics*, in press (1999)	Feb. 1998
880	Riahi, D. N.	On a turbulent boundary layer flow over a moving wavy wall	Mar. 1998
881	Riahi, D. N.	Vortex formation and stability analysis for shear flows over combined spatially and temporally structured walls—*Mathematical Problems in Engineering*, in press (1999)	June 1998
882	Short, M., and D. S. Stewart	The multi-dimensional stability of weak heat release detonations	June 1998
883	Fried, E., and M. E. Gurtin	Coherent solid-state phase transitions with atomic diffusion: A thermomechanical treatment—*Journal of Statistical Physics*, in press (1999)	June 1998
884	Langford, J. A., and R. D. Moser	Optimal large-eddy simulation formulations for isotropic turbulence	July 1998
885	Riahi, D. N.	Boundary-layer theory of magnetohydrodynamic turbulent convection—*Proceedings of the Indian National Academy (Physical Science)*, in press (1999)	Aug. 1998
886	Riahi, D. N.	Nonlinear thermal instability in spherical shells—in *Nonlinear Instability, Chaos and Turbulence* **2**, in press (1999)	Aug. 1998
887	Riahi, D. N.	Effects of rotation on fully non-axisymmetric chimney convection during alloy solidification—*Journal of Crystal Growth* **204**, 382–394 (1999)	Sept. 1998
888	Fried, E., and S. Sellers	The Debye theory of rotary diffusion	Sept. 1998
889	Short, M., A. K. Kapila, and J. J. Quirk	The hydrodynamic mechanisms of pulsating detonation wave instability	Sept. 1998
890	Stewart, D. S.	The shock dynamics of multidimensional condensed and gas phase detonations—Proceedings of the 27th International Symposium on Combustion (Boulder, Colo.)	Sept. 1998
891	Kim, K. C., and R. J. Adrian	Very large-scale motion in the outer layer	Oct. 1998
892	Fujisawa, N., and R. J. Adrian	Three-dimensional temperature measurement in turbulent thermal convection by extended range scanning liquid crystal thermometry	Oct. 1998
893	Shen, A. Q., E. Fried, and S. T. Thoroddsen	Is segregation-by-particle-type a generic mechanism underlying finger formation at fronts of flowing granular media?—*Particulate Science and Technology*, in press (1999)	Oct. 1998
894	Shen, A. Q.	Mathematical and analog modeling of lava dome growth	Oct. 1998
895	Buckmaster, J. D., and M. Short	Cellular instabilities, sub-limit structures, and edge-flames in premixed counterflows	Oct. 1998
896	Harris, J. G.	*Elastic waves*—Part of a book to be published by Cambridge University Press	Dec. 1998
897	Paris, A. J., and G. A. Costello	Cord composite cylindrical shells	Dec. 1998
898	Students in TAM 293–294	Thirty-fourth student symposium on engineering mechanics (May 1997), J. W. Phillips, coordinator: Selected senior projects by M. R. Bracki, A. K. Davis, J. A. (Myers) Hommema, and P. D. Pattillo	Dec. 1998
899	Taha, A., and P. Sofronis	A micromechanics approach to the study of hydrogen transport and embrittlement	Jan. 1999
900	Ferney, B. D., and K. J. Hsia	The influence of multiple slip systems on the brittle–ductile transition in silicon	Feb. 1999
901	Fried, E., and A. Q. Shen	Supplemental relations at a phase interface across which the velocity and temperature jump	Mar. 1999

List of Recent TAM Reports (cont'd)

No.	Authors	Title	Date
902	Paris, A. J., and G. A. Costello	Cord composite cylindrical shells: Multiple layers of cords at various angles to the shell axis	Apr. 1999
903	Ferney, B. D., M. R. DeVary, K. J. Hsia, and A. Needleman	Oscillatory crack growth in glass	Apr. 1999
904	Fried, E., and S. Sellers	Microforces and the theory of solute transport	Apr. 1999
905	Balachandar, S., J. D. Buckmaster, and M. Short	The generation of axial vorticity in solid-propellant rocket-motor flows	May 1999
906	Aref, H., and D. L. Vainchtein	The equation of state of a foam	May 1999
907	Subramanian, S. J., and P. Sofronis	Modeling of the interaction between densification mechanisms in powder compaction	May 1999
908	Aref, H., and M. A. Stremler	Four-vortex motion with zero total circulation and impulse	May 1999
909	Adrian, R. J., K. T. Christensen, and Z.-C. Liu	On the analysis and interpretation of turbulent velocity fields—*Experiments in Fluids*, in press (1999)	May 1999
910	Fried, E., and S. Sellers	Theory for atomic diffusion on fixed and deformable crystal lattices	June 1999
911	Sofronis, P., and N. Aravas	Hydrogen induced shear localization of the plastic flow in metals and alloys	June 1999
912	Anderson, D. R., D. E. Carlson, and E. Fried	A continuum-mechanical theory for nematic elastomers	June 1999
913	Riahi, D. N.	High Rayleigh number convection in a rotating melt during alloy solidification	July 1999
914	Riahi, D. N.	Buoyancy driven flow in a rotating low Prandtl number melt during alloy solidification	July 1999
915	Adrian, R. J.	On the physical space equation for large-eddy simulation of inhomogeneous turbulence	July 1999
916	Riahi, D. N.	Wave and vortex generation and interaction in turbulent channel flow between wavy boundaries	July 1999
917	Boyland, P. L., M. A. Stremler, and H. Aref	Topological fluid mechanics of point vortex motions	July 1999
918	Riahi, D. N.	Effects of a vertical magnetic field on chimney convection in a mushy layer	Aug. 1999
919	Riahi, D. N.	Boundary mode–vortex interaction in turbulent channel flow over a non-wavy rough wall	Sept. 1999
920	Block, G. I., J. G. Harris, and T. Hayat	Measurement models for ultrasonic nondestructive evaluation	Sept. 1999
921	Zhang, S., and K. J. Hsia	Modeling the fracture of a sandwich structure due to cavitation in a ductile adhesive layer	Sept. 1999
922	Nimmagadda, P. B. R., and P. Sofronis	Leading order asymptotics at sharp fiber corners in creeping-matrix composite materials	Oct. 1999
923	Yoo, S., and D. N. Riahi	Effects of a moving wavy boundary on channel flow instabilities	Nov. 1999
924	Adrian, R. J., C. D. Meinhart, and C. D. Tomkins	Vortex organization in the outer region of the turbulent boundary layer	Nov. 1999
925	Riahi, D. N., and A. T. Hsui	Finite amplitude thermal convection with variable gravity	Dec. 1999